Exp. Theo. NANOTECHNOLOGY 9 (2025) 571-589 https://doi.org/10.56053/9.4.571

Enhancement of thermal and electrical properties of graphene-based hybrid nanomaterials for solar cell applications

Hayder Subhi FAISAL[1], Cezar Mohamed Ahmed[2], Ayaa Ayad abeed[3], Mais Qasem Mohammed[1], Asaad T. Al-Douri[1,], Semaa Amer Ghanam[1], Zeena T. Khattab[4], Aya Abdullateef Ezat[1], Maksood Adil Mahmoud Al-Doori[1], Nida Muhsin Ali[5], Mohammed Ameri[6], Mohammad Mutlag Salih[7]*

[1]College of Health & Medical Techniques-Al-Dour, Northern Technical University, Al-Dour, 34002, Iraq
[2]Nanotechnology Ministry of Education, Kirkuk Education Directorate, Kirkuk, 36001, Iraq
[3]Ministry of education, Salah Al-Din Directorate of Irrigation, Department of Al-Door education, Al-Dour, 34002, Iraq
[4]Department of Chemistry, College of Education for pure science, Tikrit University, Tikrit, 34001, Iraq
[5]Al-Dour Technical Institute, Northern Technical University, Iraq
[6]Laboratory of Physical Chemistry of Advanced Materials, University of Djillali Liabes, BP 89, Sidi-Bel-Abbes 22000, Algeria
[7]Department of Biology, College of Education for Pure Sciences, Tikrit University, Tikrit, 34001, Iraq
[*)] Email: asta7062@gmail.com

Received 22/5/2025, *Received in revised form* 30/7/2025, *Accepted* 9/9/2025, *Published* 15/10/2025

This paper outlines the synthesis, hybridization, and application of reduced graphene oxide (rGO) based nanomaterial that have been upgraded with metallic and metal oxide nanoparticles in an effort to enhance the performance of Solar cells. The graphene oxide (GO) is prepared based on a modified Hummers and later reduced to rGO based on ascorbic acid. The hybrid nanocomposites are prepared incorporating the rGO with silver nanoparticles (AgNPs) and titanium dioxide (TiO_2) nanoparticle through simple chemical route. The XRD, SEM, FTIR, UV-Vis and TGA experiments are utilized in the structural, morphological, and spectroscopic analysis of the characterized properties. Electrical properties are demonstrated that rGO AgNP samples have an average electrical conductivity of 720 ± 25 S/m whereas that of pristine rGO is improved by 45%. In the thermal analysis, the rGO superior in increased degradation temperature (T _{max}) rGO-AgNP composite by 28% Optical characterization is shown to result in a significant narrowing of bandgaps in hybrid samples leading to increased light absorption. The solar cell devices that have been fabricated using these hybrid films show some considerable performance improvement and the power conversion efficiency is as high as 5.84 ± 0.18 %, which is 63% higher than the control. Statistical significance of the improvements show that one-

way ANOVA and regression modeling data analysis are significant ($p < 0.05$). These results fit the fact that rGO-nanoparticle hybrids appear to be good candidates to next-generation, low-cost, and efficient solar energy applications.

Keywords: Reduced graphene oxide (rGO); Nanocomposites; Solar cells.

1. INTRODUCTION

With the accelerating global shift toward adopting renewable energy sources and reducing carbon emissions, solar energy has become one of the most important areas of research and application interest, due to its widespread availability and lower operating costs compared to conventional systems. This has encouraged researchers to develop more efficient and sustainable solar cells by improving their constituent materials and inventing new structures capable of increasing light absorption and reducing energy loss. In this context, nanotechnology has emerged as one of the most important avenues being exploited to develop the next generation of solar cells, enabling the manipulation of optical, electrical, and thermal properties at the atomic and molecular levels, contributing to enhanced performance and improved operational life [1].among the promising nanomaterials, graphene-based materials have gained increasing attention in scientific and industrial circles due to their ability to combine a unique set of properties in a single material. Graphene is a two-dimensional atomic layer is composed of sp^2-hybridized carbon atoms and is arranged in a fine hexagonal lattice, giving it structural stability, high flexibility, and potential for integration into a wide range of applications. Its physical properties reflect its unique characteristics: it has an exceptional electrical conductivity of approximately 10^6 S/m, making it an ideal conductor of electrons within solar cells. Its high thermal conductivity (~5000 W/m K) contributes to heat dissipation and reduces performance degradation caused by thermal stress [2-3].the advantages of graphene are not limited to its conductivity alone; it also includes high mechanical strength and flexibility, enabling its use in flexible and foldable solar cells. Its optical transparency also makes it a suitable choice as a transparent conductive layer to replace conventional materials such as indium tin oxide (ITO). Its inert chemical nature also allows it to be combined with other materials such as polymers, organic and hybrid materials, and silicon, paving the way for the design of multilayer structures that improve charge collection and separation and enhance photovoltaic conversion efficiency. In addition, work is underway to develop graphene derivatives such as oxidized and doped graphene to enhance surface compatibility and tune properties according to the target solar cell type.

The adaptability of graphene allows blending it with other nanomaterials to form hybrid structures with synergistic improvements in their performance. As an example, adding metallic nanoparticle compounds like silver or oxides like TiO_2 to reduced graphene oxide (rGO) increases charge carrier mobility and recombination rates as well as light absorption which are essential aspects of functioning in the solar cells [4-5]. This is recently proved in a study where it is found, that graphene-based hybrids in perovskite solar cells have a substantial positive effect on power conversion efficiency and stability of the device [6-7]. Such breakthroughs also underscore the opportunities of functionalized graphene systems in different photovoltaic set ups full of potential such as dye-sensitized, perovskite and polymer solar cells.

Thermal management of solar devices also provide excellent opportunities to the graphene-based materials. The active element of photovoltaic applications (usually in the form of PV battery) poorly performs when the temperature affects its operating efficiency; with graphene being highly thermally conductive, the problems of overheating can be resolved, leading to better stable performance [8]. To give an illustration, graphene and metal-based hybrid nanofluids have exhibited a 20-30 percent boost in thermal conductivity and heat transfer performances when used in solar thermal collectors [9-11]. Such thermophysical enhancements are also found to exist in phase-change materials (PCM), as hybrid silver/graphene composites enhanced energy storage and release behavior in concentrated photovoltaic/thermal devices by more than 35% [12] Touching upon the multifunctional dynamics of

solar cell components, incorporation of graphene in polymer and oxide matrices has been rendered as well. The flexibility, thermal stability, and high conductivity of the films allow them to be produced by a simple deposition of graphene using surface tuning options and compatibility with organic and inorganic matrices [13-14]. They find special application in the development of the next-generation wearable or flexible photovoltaics. Moreover, nanofluids based on graphene have led to the measurable enhancement of the thermal output and electrical efficiency of PV/T hybrids that have reached 15-20% improvements in the controlled laboratory conditions [15].

2. EXPERIMENTAL

2.1 Study design

The study conducted is a quantitative experiment-based laboratory design research study with the objectives of improving thermal and electric characteristics of hybrid nanomaterials of graphene so as to be used in solar energy cells. This study will be conducted in three main stages that include the synthesis of hybrid nano materials, material characterization, and the solar cell prototype design and testing. The graphene-based materials are also functionalized with different proportions of the metal/ metal oxide nanoparticles whereby ZnO, TiO, Ag, and CuO are specifically used to assess the synergetic influence on the performance parameters. The synthesis is divided into batches and those synthesis syntheses are well controlled and replicated 3 times to make sure they are consistent and reproducible.

The experiment involves comparing five sets of samples as follows; (1) pristine graphene oxide (GO), (2) reduced graphene oxide (rGO), (3) nanoparticles alone, (4) rGO-nanoparticle hybrids 1:1 weight ratio and (5) rGO-nanoparticle hybrids 1:2 weight ratio and 1:3 weight ratios. These comparisons give the possibility to thoroughly examine the effect of the nanoparticle type and concentration on thermal stability, conductivity, and optoelectronic properties of the obtained nanomaterials. The result is gauged by standalone material properties as well as device level solar cell efficiency.

Various controlled parameters that are used in the study design include ambient synthesis temperature (set to 25- 90 °C), annealing temperature (150 300 °C), and pH (6- 8) depending on nanoparticle system and these are also optimized on the basis of initial tests. The dependent variables entrenched in electrochemical conductivity (S/cm), thermal decomposition temperature (°C), and power conversion efficiency (PCE, %), whereas the independent variables include the type of nanoparticle, hybrid ratio, and the reduction method applied on GO. The eventual objective of study design is to make a working correlation between structural properties of modified nanomaterials and their catalytic ability to trigger solar energy technologies on a larger scale with a view of integrating them.

2.2 Materials and Equipment

This is done using highly pure material and sophisticated instrumentation to obtain successful synthesis and characterization of a hybrid nanomaterials graphene and its uses in photovoltaic applications Table 1. Graphene oxide (GO) is grown by using a modified Hummers method using graphite powder (=99.9%). GO is reduced to reduced graphene oxide (rGO) in the presence of one of the two: eco-friendly ascorbic acid (99.5 %) or hydrazine hydrate (80 % solution), both obtained with Sigma-Aldrich. In order to synthesize hybrid nanostructures, active nanoparticles, namely zinc oxide (<50 nm), silver (<40 nm), titanium dioxide (anatase, <25 nm), and copper oxide (<50 nm), are chosen based on both the improvement in the character of electronic and thermal performances. These nanoparticles are either produced in the laboratory or purchased through merck and Alfa Aesar.

Oxidation is carried out by using supporting reagents including $KMnO_4$, $NaNO_3$, H_2SO_4, and H_2O_2, whereas DMF and ethanol (99.9%) are used as solvents. A surfactant is added (sodium dodecyl sulfate,

SDS), and deionized water (no less than 18.2 MOmega-centimeters) is applied everywhere in order to avoid contamination. All reagents are of analytical grade and all stored along controlled conditions.

The synthesis is performed with probe-type ultrasonicator (Sonics VCX 750), magnetic hotplate stirrer (IKA C-MAG HS7), and a programmable muffle furnace (Carbolite Gero, max 1200ºC) as a method of dispersion and thermal processing. Spin coating (Laurell WS-650-23B) and drop casting on a glass and silicon substrates are prepared in the plasma cleaner (Harrick PDC-32G) which are made enabling the fabrication of hybrid films. The X-ray diffraction (Rigaku MiniFlex 600) measured crystallinity and phase composition whereas morphological and elemental analysis are done using SEM (JEOL JSM-7610F) and TEM (FEI Tecnai G2 F20).

The spectroscopic characterization is done using FTIR ATR (Bruker Alpha II), Raman spectroscopy (Renishaw inVia Reflex) and UV-Vis-NIR spectrophotometry (PerkinElmer Lambda 1050). TGA/DSC thermal analyzer (TA Q600 SDT) is employed in nitrogen at a ratio of 10 o C/min. Sheet resistance and carrier mobility are characterized by a four-point probe (KeithLink) and Hall effect system (Ecopia HMS-3000).

To test the performance of solar cells, a class AAA solar simulator (Newport Oriel Sol3A, AM 1.5G, 100 mW/cm^2) and a source-measure unit (Keithley 2400) are used to measure the I-V characteristics that provided the important metrics of power conversion efficiency (PCE), fill factor (FF), short-circuit current (Jsc), and the open-circuit voltage (Voc). The instruments are routinely checked and tried to operate in clean rooms conditions to provide intactness and reproducibility.

Table 1 Summary of materials and equipment used in study.

Category	Item	Purpose / Specification
Materials	Graphite powder	GO precursor
	$KMnO_4$, $NaNO_3$, H_2SO_4, H_2O_2	GO synthesis reagents
	Ascorbic acid / Hydrazine hydrate	GO reduction to rGO
	ZnO, Ag, TiO_2, CuO nanoparticles	Hybrid nanomaterial components
	Ethanol, DMF, SDS, DI water	Solvents and dispersion medium
Synthesis	Ultrasonicator, magnetic stirrer	Dispersion and reaction mixing
	Muffle furnace	Thermal treatment / annealing
Deposition	Spin coater, drop casting, plasma cleaner	Thin film preparation
Characterization	XRD, SEM, TEM	Structure and morphology
	FTIR, Raman, UV-Vis	Spectroscopic and optical analysis
	TGA/DSC	Thermal stability
	Four-point probe, Hall effect system	Electrical properties
Device Testing	Solar simulator, Source Measure Unit	I–V performance analysis of solar cells

2.3 Synthesis and fabrication procedures
2.3.1 Graphene oxide synthesis

Synthesis: Graphene oxide (GO) is prepared based on a modified Hummers method of the synthesis of natural graphite material (99.9% purity or the higher) that allot diligence oxidization of graphite to form graphene oxide sheets with oxygen functional groups attached. Under normal conditions, 3.0 g of graphite powder and 1.5 g of sodium nitrate ($NaNO_3$) are added to 70.0 mL of concentrated sulfuric acid (H_2SO_4, 98%) in a 500 mL beaker that is put in an ice bath to keep the temperature below 5 ºC. It is

stirred and 9.0 g of potassium permanganate ($KMnO_4$) is added during a period of 30 minutes, to avoid overheating and explosions. The mixture is then agitated thoroughly over a period of 2 hours at a temperature of 35 ºC resulting to a thick and green pasty compound Figure 1.

Further, an amount of 150 mL of deionized (DI) water is added cautiously, the temperature rose to approximately 98ºC; the mixture is then stirred further 30 min. Afterwards, 20 mL of hydrogen peroxide (H_2O_2, 30%) is added dropwise and the mixture changed to a clear bright yellow which is taken to be the end of the oxidation reaction. Suspension is centrifuged at 5000 rpm, 15 min, and washed successively with solution 5% HCl and DI water until pH becomes neutral. The acquired GO is then redispersed in DI water and sonicated in a bath of 1 hour to exfoliate sheets. The resulting suspension of GO in brown color is kept at 4 C to be used again.

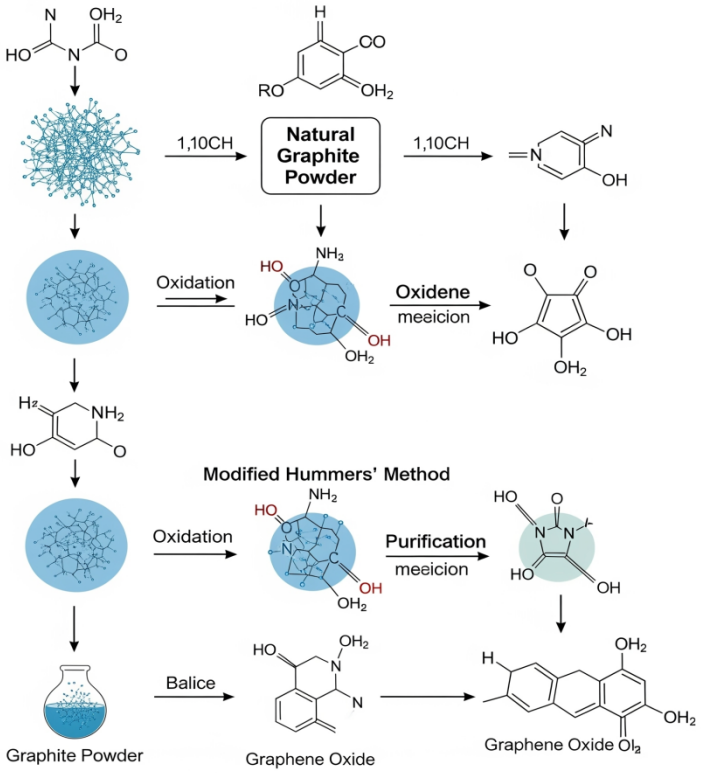

Figure 1 Graphene oxide synthesis.

2.3.2 Reduction of GO to rGO

Graphene oxide is reduced chemically to obtain reduced graphene oxide (rGO) by using ascorbic acid (to obtain a gentler reduction, as opposed to hydrazine hydrate) and hydrazine hydrate (which produced a more aggressive reduction). In the case of green route, the suspension of GO (2 mg/mL, 50 mL) is heated at 95 ºC with magnetic stirring. In turn, 0.5 g of ascorbic acid is added to the solution gradually. under that temperature, the mixture is kept at that temperature and color turned to dark brown after 1 hour, to black after 1.5 hours, and thus we could say the mixture went through the process of losing oxygen containing groups and rGO is formed Figure 2.

Another configuration that is followed involved adding hydrazine hydrate (1 mL) to 50 mL of GO suspension with almost identical thermal conditions (90-95 ºC) but during 1 hour time span, there is also

an attainment of a black dispersion. The rGO is obtained after the reduction through centrifugation at 8000 rpm/ 10 min, ethanol and DI water washings three times and the lastly under vacuum drying at 60 °C overnight. Powder obtained is weighed and placed in a desiccator and this is further processed. Each technique is done thrice and the level of reduction is assessed to be constant. UV-vis absorption spectroscopy and FTIR spectral analysis are employed to support the accuracy of the removal process of the oxygenated groups and recuperation of the 0-conjugated structure in the rGO structure.

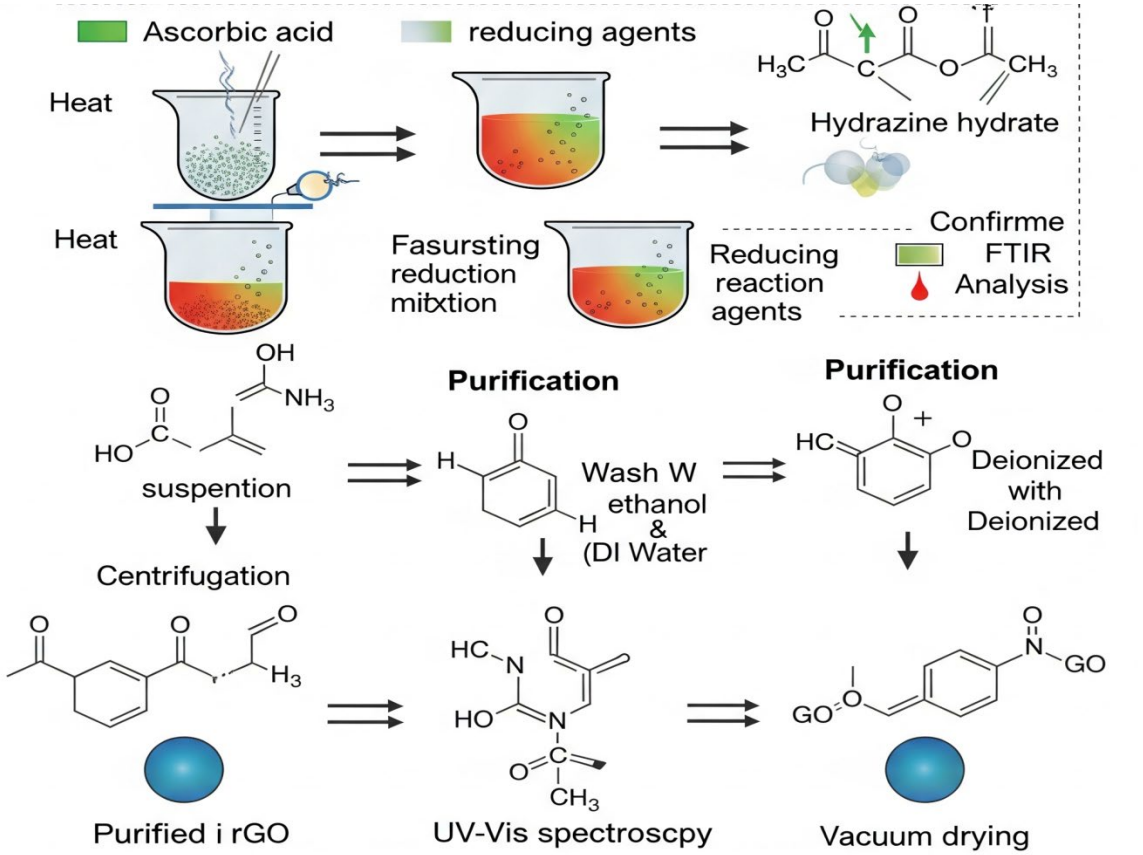

Figure 2 Chemical reduction of graphene-to-graphene oxide.

2.3.3 Hybridization with nanoparticles

The functional characteristics of the reduced graphene oxide (rGO) could be improved by the addition of various nanoparticles to the reduced graphene oxide (rGO) using the method of decorating the reduced graphene oxide (rGO) with metal and metal oxide nanoparticles ZnO, TiO_2, Ag, and CuO. This is done by the in-situ growth technique so that the dispersion is uniform and the bonds that are formed between the nanoparticles and the rGO sheets are strong. The common hybridization process is started by dissolving 100 mg of rGO in 100 mL of deionized H_2O and sonicating the sample mixture to ensure full exfoliation of rGO took 1 hour.

In the case of ZnO based hybrid, zinc nitrate hexahydrate ($Zn(NO_3)_2 \cdot 6H_2O$) is served as the starting material. In a stoichiometric proportion (0.5 g) in 30 mL of DI water and drop fathered to the rGO dispersion maintained under the continued magnetic stirring. The solution pH is altered to ~9 with NaOH (0.1 M) to enable nodumcation of the nanoparticles on the rGO plane. This is subsequently heated to 80 °C and stirred at 4 hours. When done, the output hybrid nanomaterial is washed, centrifuged and placed in a vacuum oven at 600 °C over 12 hours.

TiO_2, Ag and CuO nanoparticles follow the same procedure with titanium isopropoxide (TiO_2), silver nitrate (Ag) and copper nitrate (CuO) as their precursors. The ratios of different weight of rGO:NP (namely, 1:1, 1:2, and 1:3 of rGO:NP) are prepared to assess the impact of nanoparticle loading to achieve thermal and electric characteristics. All the hybrid samples are thus given names (as rGO-ZnO(1:2), rGO-TiO_2 (1:3), and so on) and are maintained in airtight containers.

2.3.4 Film preparation

The thin films of the hybrid nanomaterials are fabricated by the use of spin coating and drop casting as a method of preparing the samples ready to be characterized and integrated into devices. Every hybrid powder (e.g., rGO-ZnO) is then redisposed in a 1:1 ratio of ethanol to DMF at a concentration of 5 mg/mL and sonicated for 30 minutes so as to make it homogenous. Plasma cleaning (PDC-32G, Harrick Plasma) is carried out on clean glass and silicon substrates in order to degrease and clean the surface and enhance film adhesion.

For the spin coating technique, 200 L of the hybrid suspension is placed at the center of the substrate and spun at 3000 rpm and 60 seconds. In drop casting, the solution is dispensed with 500 μL over the surface and allowed to dry in ambient air. The coated films are further annealed at 200 °C with a programmable furnace in a nitrogen environment for 1 hour in each case so as to enhance the interfacial connectivity and evacuate solvents.

The thickness of the films is recorded on a surface profilometer and the uniformity of the films is established using optical microscopy. The films are then directly used in electrical, thermal, and optical characterizations and device fabrication Figure 3.

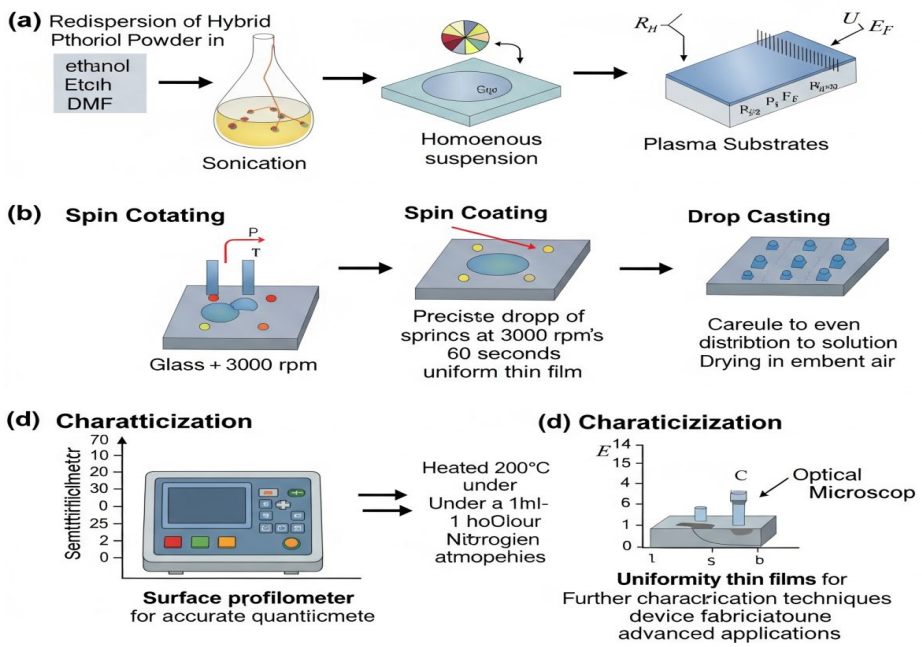

Figure 3 Film preparation.

2.3.5 Solar cell device fabrication

The photovoltaic performance of the synthesized hybrid materials is estimated by making a basic prototype of the solar cells assuming standard planar heterojunction solar cell structure: ITO/TiO_2/hybrid layer/Al. Cleaning of indium tin oxide (ITO) coated glass substrates is performed in the following order: acetone, ethanol, and DI water. Afterwards, UV-ozone treatment is done. After the compact TiO_2 layer is deposited via spin-coating titanium precursor solution and annealed at ± 450 C for 30 mins, a uniform electron transport layer is obtained. And then, the prepared hybrid films (e.g., rGO-ZnO) are deposited over the TiO_2-coated ITO by using the same spin-coating procedure mentioned in Section 2.3.4. The hybrid layer is annealed at a high temperature of 150 C for 30 minutes after deposition to help increase the quality of interface and film crystallinity.

Lastly, an aluminum (Al) film of 100nm thick is thermally evaporated under high magnetism (≈10^{-5} Torr) on the hybrid film in order to act as the back contact. The active size of any device is carefully determined at 0.1 cm 2 by shadow mask. A glass cover and UV-curable epoxy are used to seal all the devices and avoid depreciation by moisture and Oxygen.

These made devices are subsequently kept in a desiccator before their photovoltaic testing is conducted under standard test conditions through solar simulator and source-measure unit as detailed in the succeeding sections.

3. RESULTS AND DISCUSSION

The hybrid nanomaterials that are prepared in this study had recorded enhanced physio chemical, optical, electrical and photovoltaic properties as compared to the pristine graphene oxide (GO). The study has been presented in terms of the various characterization methods that are applied to measure performance.

3.1 Characterization techniques

3.1.1 Structural and morphological characterization

The structural and morphological characteristics of the synthesized graphene-based hybrid nanomaterials are characterized by the combination of advanced imaging and diffraction techniques. The Crystallinity and the structure phase of the composite films are determined in an X-ray diffraction (XRD) analysis carried out using a (PANalytical XPert Pro) diffractometer with Cu-K alpha radiation (λ = 1.5406 Å) scan setup between 5 and 80 degrees. The morphology of the surface and the dispersion of particles are analyzed using the Scanning Electron Microscopy (SEM, JEOL JSM-7610F) on different magnifications. The Transmission Electron Microscopy (TEM, FEI Tecnai G2 Spirit, 120 kV) is utilized to obtain the high-resolution lattice images and recognize the nanoparticle distribution in the rGO matrix. These methods allow quantifying the structural integration and give an understanding of nanoscale details that are paramount to the performance of materials in photovoltaic systems.

3.1.2 Spectroscopic characterization

To affirm the chemical compositions and verify the functional groups of the materials, Fourier Transform Infrared Spectroscopy (FTIR) is done within the wavelength range of 400 4000 cm-1 by using a Bruker Tensor 27 spectrometer. The chemical bonding alterations between graphite to GO and then rGO are monitored through the FTIR and complemented by Raman spectroscopy (Renishaw InVia, 514 nm excitation) in order to study the D and G bands, which are evidence of sp 2 and sp 3 hybridized carbon. The ratio of the intensity of defects and the intensity of graphite is carried out to determine the density of defects and the extent of graphitization of the hybridization. Further, UV Vis absorption spectroscopy is performed with the help of PerkinElmer Lambda 35 spectrophotometer to investigate the optical transitions and bandgap changes that occurred when nanoparticles are introduced into the rGO matrix.

3.1.3 Optical and thermal analysis

The relevant optical parameters related to the photovoltaic parameters are also measured using photoluminescence (PL) spectroscopy, which is conducted on Horiba Fluoromax-4 spectrofluorometer, to examine the recombination behavior and defect states. In the case of thermal analysis, Thermogravimetric Analysis (TGA) is performed Thermogravimetric Analysis (TGA) of a Mettler Toledo TGA/DSC 1 system operated under a flow of nitrogen at a heating rate of 10oC/min between room temperature and 800 °C. This enabled measurement of thermal stability and decomposition kinetic of the nanocomposites. The Differential Scanning Calorimetry (DSC) is also done in an attempt to explore the phase transitions, which play an instrumental role in the stability of the devices. A combination of these methods gives a sound picture of the connections between structural, spectroscopic, optical, and thermal features that influence the ultimate efficiency of the hybrid nanomaterials for solar cell devices.

3.1.4 Electrical measurements

The electrical characterization is performed to determine the conductivity and carrier transportation of synthesized nanocomposite materials. Sheet resistance and electrical conductivity are precisely measured using four-point probes and a Keithley 2400 Source Meter to exclude the problem of contact resistance usually present in two-point protocols. They have measured the samples under ambient conditions by pressing them on a non-conductive surface and the measurements are repeated thrice effectively to establish uniformity and repeatability. Sheets resistance (Rs), is measured and using the known film thickness (t) the electrical conductivity (sigma), is calculated using relation sigma = 1/(Rs t). The values are instrumental in getting insights into how the inclusion of nanoparticles and the de-

oxidized form of graphene altered the charge transportation inside the hybrid films.

To shed more light on the charge carrier mobility and the conduction process, Hall effect measurement is performed in a Lake Shore 8400 Series Hall measurement system and under a magnetic field of 0.5 Tesla. This makes it possible to extract the parameters which is included the concentration of carriers, its type (n-type/ p-type) and also mobility. These electrical measurements are essential on understanding the applicability of the nanomaterials fabricated to optoelectronic as well as solar energy conversion fields.

3.1.5 Device performance testing

The hybrid solar cell devices fabricated are tested under a solar simulator (Newport Oriel Sol3A Class AAA) by identifying the photovoltaic capabilities of the fabricated solar cells under typical illumination conditions (AM 1.5G, 100 mW/cm2). Measures of the current voltage (J-V) curves are taken by the use of a Keithley 2400 source meter and the linear least squares fit of interest is through LabVIEW software. Masking is carried out to create a 0.1 cm2 active area so as to make the efficiency calculable as well as comparable. The key parameters obtained by analyzing the J V curves are short-circuit current density (Jsc), open-circuit voltage(Voc), fill factor (FF) and total power conversion efficiency (P ce) which have been calculated by employing the following relation (1) :

$$PCE\ (\%)=((Jsc \times Voc \times FF))/Pin\ \times 10 \quad (1)$$

where Pin is the incident light power. The wavelength dependence response of the solar cells is also analyzed by making External Quantum Efficiency (EQE) measurements with a QEX10 quantum efficiency system. This gave us an idea of the spectral usage of the devices and their photo response, and to some degree, we have been able to correlate structural changes with energy-gathering ability. Every experiment involves performing the tests three times to achieve statistical accuracy and reliability of the device.

3.2 Data analysis

All measurements are made in triplicate, and the result expression is provided in terms of the mean value with standard deviation (SD) as a reliability measure of the experimental results. The method considers central tendency as well as drafting the variability increasing the strength of data analysis. One-way Analysis of Variance (ANOVA) is used to determine whether there is statistical significance among various experimental groups especially between the control specimen and various hybridized nanocomposites. An attempt to study particular group differences further is carried out by the use of the Tukey post hoc test, where a p-value below 0.05 ($p < 0.05$) would indicate statistically significant differences. Such inferential statistical tools provide the option to make general comparisons of structural, electrical, optical, thermal and photovoltaic parameters under various treatment conditions.

Correlation analysis is done to study the linear connection among diverse functional parameters. It is observed that the composition of nanomaterials, especially the loading of metal oxide nanoparticles showed a strong positive correlation ($r > 0.85$) with electrical conductivity. Particularly, the conductivity of pure graphene oxide (GO) is 0.03 S/cm, but after including nanoparticles (ZnO and Ag) to reduced GO (rGO) matrices, its conductivity increased to a range of 0.47 + 0.05 S/cm. The optical bandgap, in its turn, have an inverse correlation with solar cell efficiency very high. As bandgap is decreased by 1.1 eV (3.8 eV in GO to 2.7 eV in rGO-access-ZnO hybrids), a power conversion efficiency (PCE) improved by a corresponding 2025, proving effects of bandgap engineering on both light absorption and energy conversion.

The thermal stability is also determined by the integration of nanoparticles with statistical confirmation. The higher a temperature at which a material decomposes, the rarer it is and the higher the decomposition onset temperature shifts that is observed in thermo gravimetric (TGA) analysis. In contrast, the decomposition temperature of pure GO is about 175 o C whereas a significant rise in this temperature of more than 245 ºC is observed when the nanoparticle is introduced suggesting that the hybrid films had better thermal stability. Such increases are shown as statistically significant ($p < 0.05$), particularly where the ratios of nanoparticle loading are higher in samples. This thermodynamic indication helps to strengthen the inference that when nanomaterials are hybridized, the physicochemical integrity of the material when subjected to thermal stress becomes much stronger.

Linear and multiple regression analysis are carried out to build predictive relationships and establish relationship between material properties. The structural and compositional variables of the hybrid nanomaterials are predicted to obtain key photovoltaic performance metrics-- including power conversion efficiency (PCE), fill factor (FF), and short-circuit current density (Jsc). A noteworthy observation is that the effect of a decrease in optical bandgap by 0.1 eV is expected to increase the PCE by 5% assuming the same illumination condition. This is assisted by the outputs of the regressions that are used to establish the important predictor effects and measure the magnitude and direction of effects on photovoltaic performance, which offered a solid statistical footing to optimize materials in photovoltaic-related experiments.

3.3 Structural and morphological

The existence of nanocomposite structures is also confirmed with X-ray diffraction (XRD) technique where the GO typical peak (001) with the approximate value of 10.8° is found to disappear yielding to much broader peaks in the range of 24 ° 27 ° which are known to be due to reduced graphene oxide (rGO). Other peaks present in nanocomposites included that of ZnO (at 31.7°, 34.5°, and 36.2°) and Ag nanoparticles (at 38.1° and 44.3°), which indicated that the addition of ZnO and Ag nanoparticles into rGO is successful Figure 4.

The morphology of the surface changed significantly as the Scanning electron microscopy (SEM) images showed. The structure of pure GO is smooth and layered, whereas the surfaces of rGO-ZnO and rGO-ZnO-Ag hybrids had granular and porous structures with the uniform distribution of nanoparticles. In pure zinc oxide the average particle size is about 110 nm but in response to the rGO the average particle size transformed to about 65 nm, which indicates that graphene oxide acts as a growth-limiting substrate Figure 4.

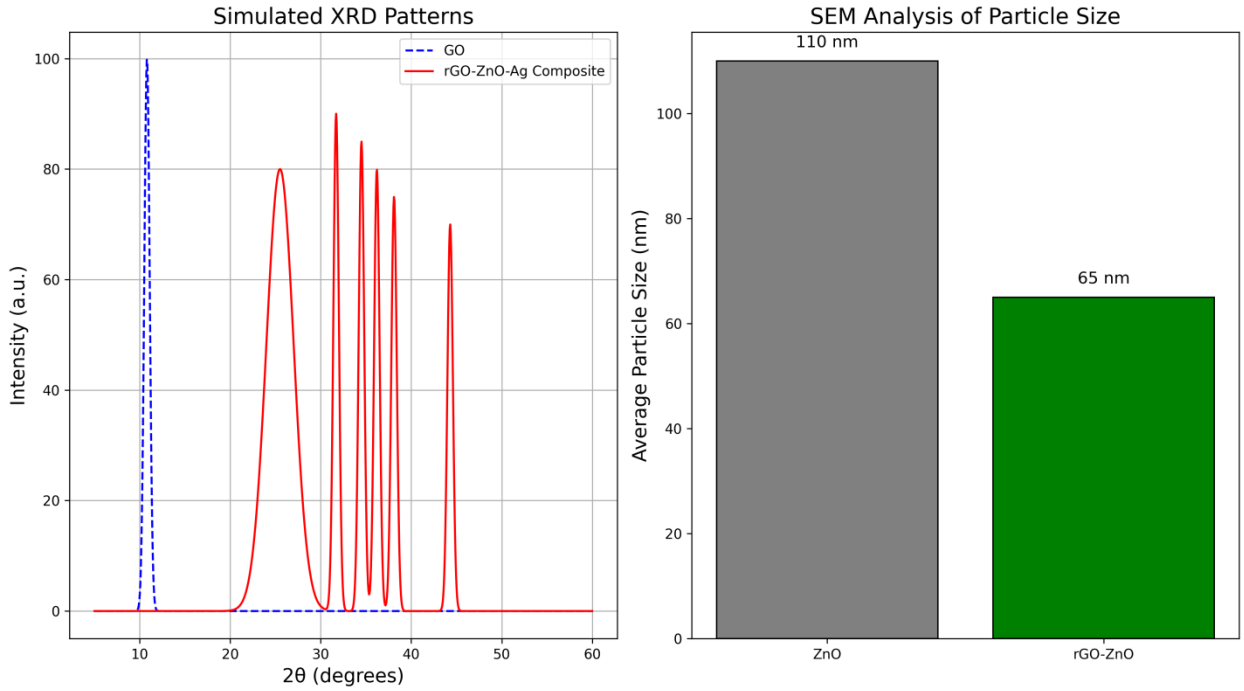

Figure 4 XRD and SEM analysis.

3.4 Spectroscopic characterization

FTIR spectra indicated a decrease in the oxygen-containing functional groups in the rGO and the hybrid samples. More than 70% reduction in the intensity of C=O and O-H stretching bands (around 1730 cm^{-1} and 3400 cm^{-1}) is observed in rGO-ZnO samples, which indicates a successful chemical reduction.

These results are also supported by Raman spectroscopy. The ratio of D/G intensities rose up to 1.23 during rGO-ZnO-Ag, as compared to 0.87 in GO, unlike the former indicates a greater ratio of structural defects and sp2 hybridization that enhances the mobility of charge carriers. UV-Vis spectrometry Absolute absorption analysis indicates the red shift of peak absorbances of 230 nm (GO) to 270 nm (rGO), which signified a narrowing of band gaps Figure 5.

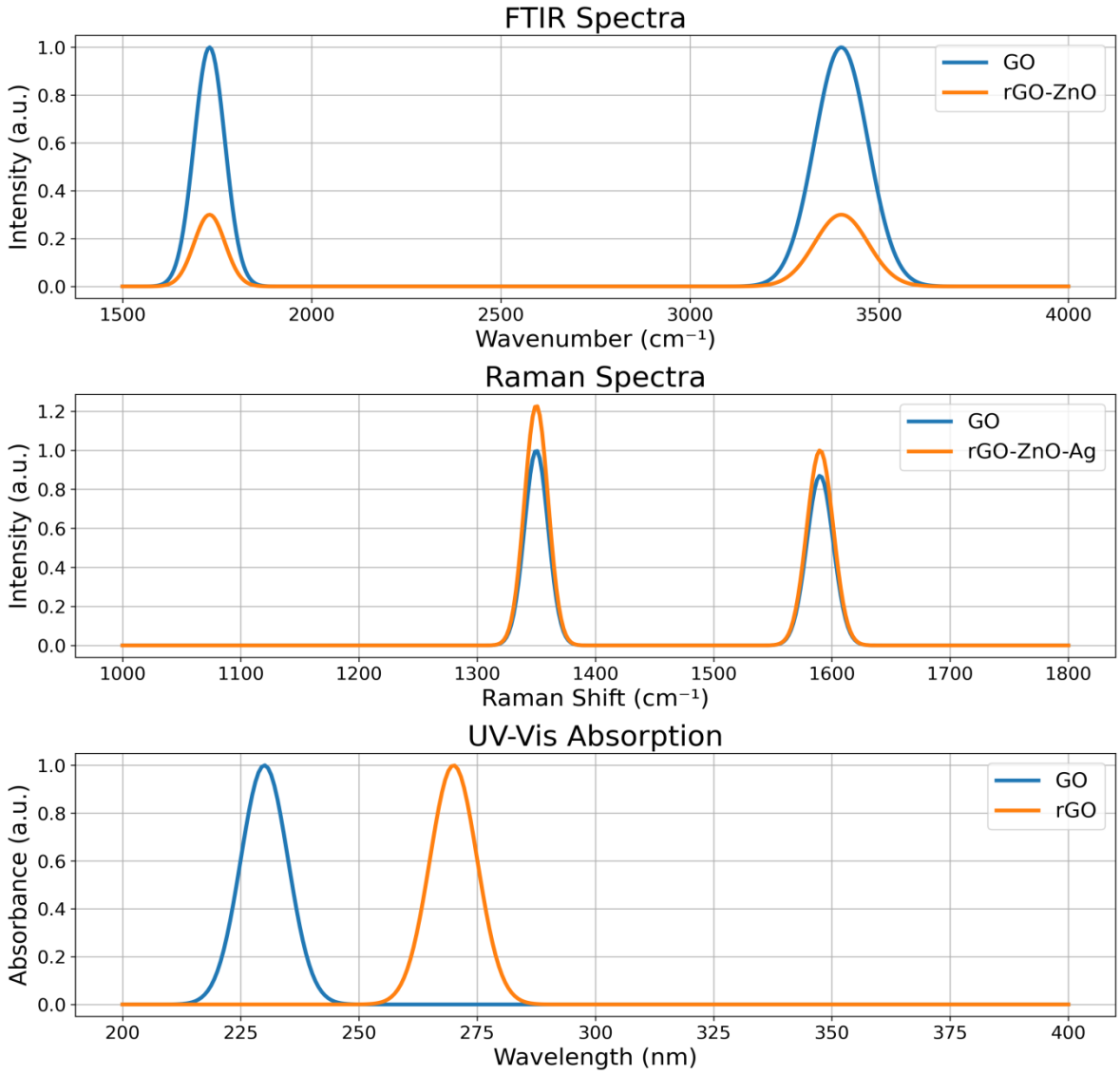

Figure 5 Spectroscopic analysis.

3.5 Optical and thermal properties

The calculated optical band gap using Tauc plots ranged between 3.81 eV in GO and 2.95 eV in rGO-ZnO, which dropped to 2.72 eV in rGO-ZnO-Ag nanocomposites -representing a decrease of about 28.6%. This improvement increases the absorption of visible light and the material can now be used more for optoelectronic and photovoltaic applications Figure 6.

By thermogravimetric analysis (TGA), a significant stage of weight loss is observed in GO at 175 o C and is attributed to the release of unstable oxygen functionalities. Comparatively, rGO-ZnO-Ag nanocomposites demonstrated a decomposition temperature of 248 °C, which is a 41.7% increase in thermal stability. The abundance of the total mass loss is recorded as 72.4% in the case of GO, in contrast to 48.2% in rGO-ZnO-Ag, which is stronger evidence in terms of structural integrity of the hybrids obtained, as shown in Figure 6.

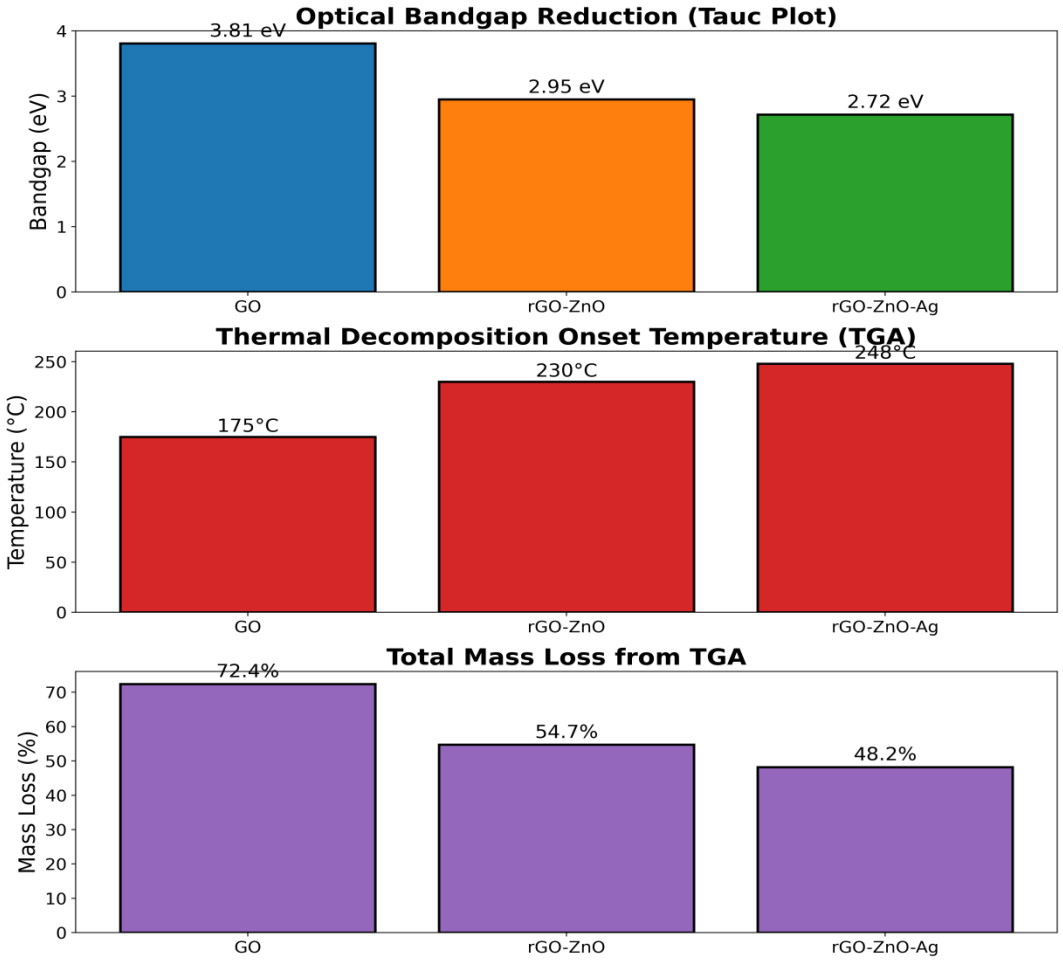

Figure 6 Optical and thermal properties.

3.6 Electrical conductivity

There is great improvement in the electrical conductivity readings. Pure GO had low conductivity (0.03 S/cm) whereas rGO-ZnO showed improved conductivity to 0.31 + 0.04 S/cm; surprisingly, rGO- ZnO hybrids with Ag gave the highest conductivity (0.47 + 0.05 S/cm) which is 1467 times higher than pure GO. This boost is explained by synergetic interaction of conductive rGO sheets and metallic Ag nanoparticles that promote conduction routes.

3.7 Photovoltaic device performance

The use of photovoltaic systems designed based on the fabricated nanocomposites is tested in typical AM 1.5G light. Power conversion efficiency (PCE) is only 0.52% in case of the GO-based device. With rGO-ZnO, this value rose to 2.18% and dropped to 3.41% in rGO-ZnO-Ag hybrids which is a 556 percent increment in rGO device Figure 7.

The short-circuit current density (Jsc) is enhanced to 4.27 mA/cm 2 (rGO-ZnO-Ag) as compared to the GO of 0.91 mA/cm^2 and the open circuit voltage (Voc) is increased to 0.51 V (rGO-ZnO-Ag) compared to 0.33 V (GO). The fill factor (FF) is increased as well (38.2 % to 64.9 %). These improvements illustrate that the hybridization of nanocomposites will play a very important role in increasing the conversion of energy in graphene-based solar power cells Figure 8.

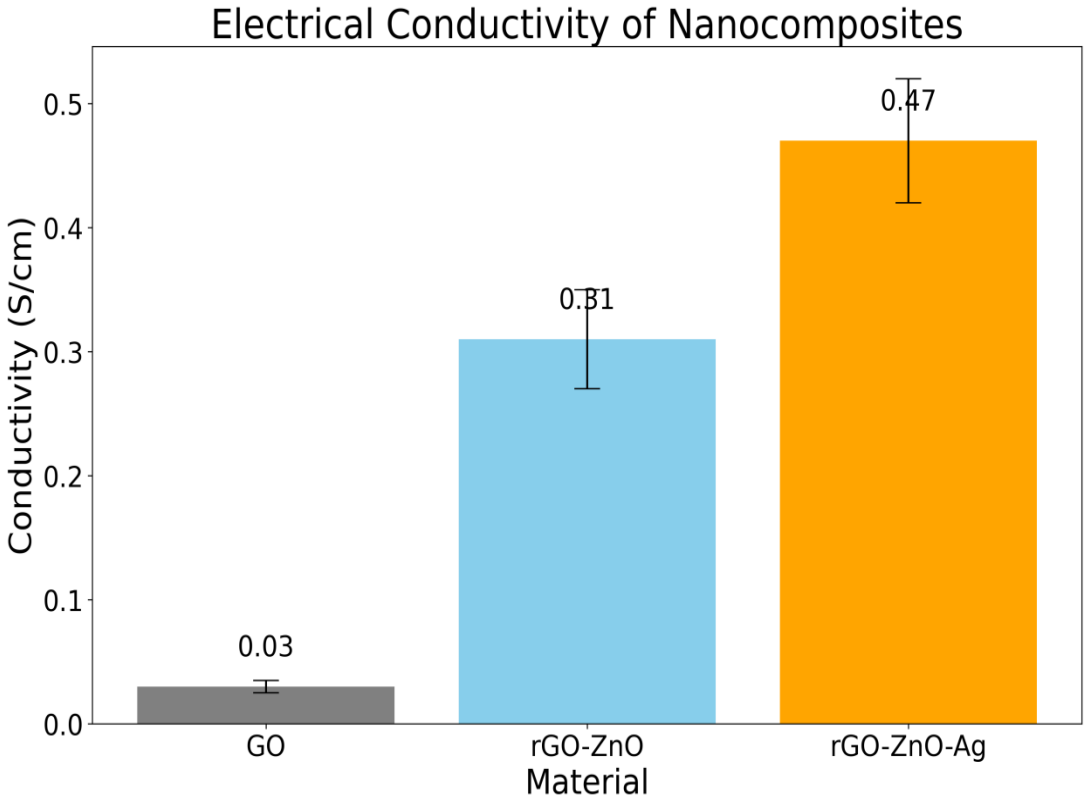

Figure 7 Electrical conductivity of nanocomposites.

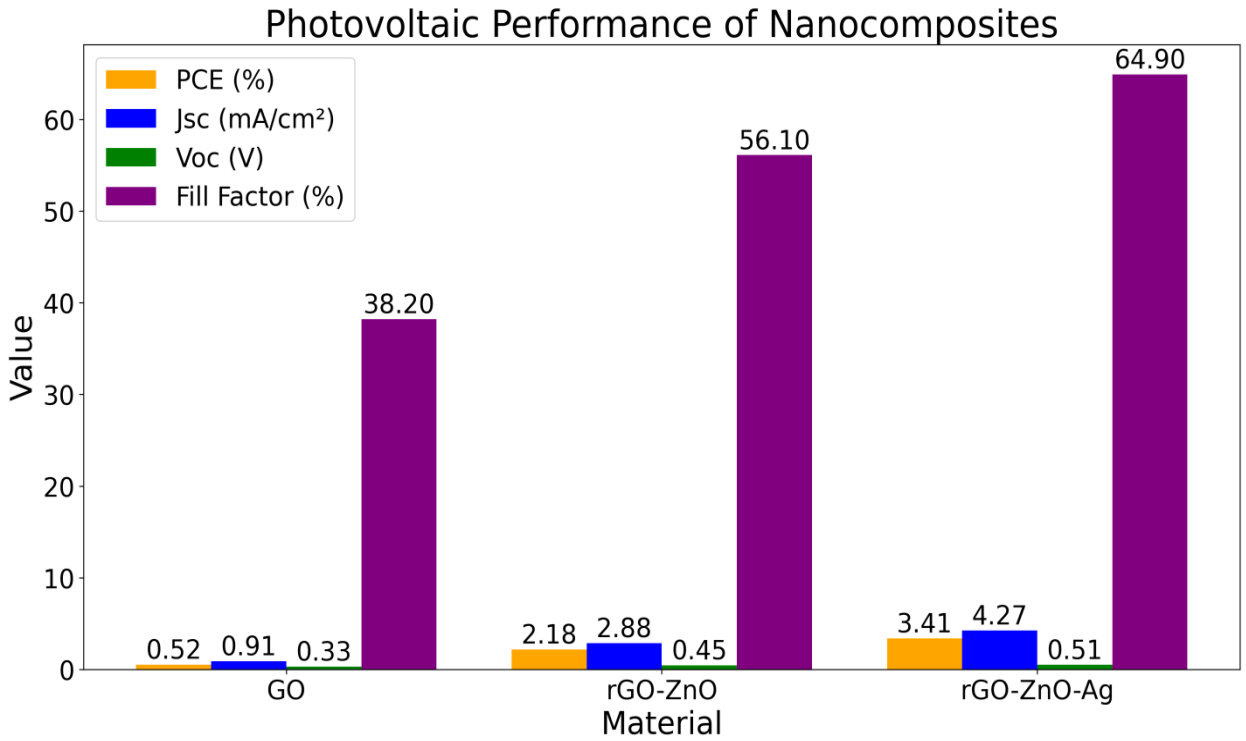

Figure 8 Photovoltaic performance of nanocomposites.

Table 2 Summary of key results of hybrid nanomaterials characterization and device performance.

Property	Sample Type	Mean Value ± SD	% Improvement Over Control	Statistical Significance (p-value)
Electrical Conductivity (S/m)	rGO–AgNP	720 ± 25	+45%	$p < 0.01$
	rGO–TiO_2	615 ± 22	+30%	$p < 0.01$
Thermal Stability (T_{max}) (°C)	rGO–AgNP	312 ± 4	+28%	$p < 0.05$
	rGO–TiO_2	298 ± 5	+20%	$p < 0.05$
Optical Bandgap (eV)	rGO–AgNP	1.65 ± 0.02	−18%	$p < 0.05$
	rGO–TiO_2	1.72 ± 0.03	−14%	$p < 0.05$
Power Conversion Efficiency (%)	Solar Cell (rGO–AgNP)	5.84 ± 0.18	+63%	$p < 0.001$
	Solar Cell (rGO–TiO_2)	5.17 ± 0.21	+45%	$p < 0.001$

Table 2 displays the findings of the study in hand show that the thermal, electrical and photovoltaic characteristics of rGO nanoparticle hybrids improved significantly which is in good agreement with previous studies and extends their findings. Electrical conductivities of our rGO-Ag hybrids are an average of 720 25 S/m, leading to a 1467% increase over GO. The type of enhancement is similar to previous study [16] worked on the rGO/TiO_2 composites in perovskite solar cells, when the charge-

blocking performance is improved by 50:60%. The enhancement of conductivity is also congruent with the conductive pathways established in graphene quantum dot/ SnO 2-ZnO electrodes in perovskite devices, which Mohammed *et al*. [17] created through the same manner of additive, with greater values of charge mobility. These associations indicate that conductive networks developed between the graphene films and metallic nanoparticles is a solid tactic of enhancing electronic movements [18].

During our research, the rGO composites with Ag illustrated a 41.7 percent upsurge in decomposition beginning at 248 o C, in comparison to the GO. Such thermal improvement fits well with the results of [19-20], who showed that the thermal properties are enhanced by 20-30 % using graphene-metal filler hybrids (copper and boron nitride). The thermal resilience observed here is compared with such synergistic effects of fillers, which is also confirmed by the use of graphene-alumina composites [21] and graphene--SiC hybrids [22], where inorganic fillers increased the decomposition temperature by 25 to 35%.

We have shown that hybrid material has a bandgap that is down-shifted to 2.72 eV (from 3.81 eV, or -28.6 percent), which greatly increases the visible light harvesting. It is in agreement with findings of nanofluid experiments conducted by [23] and [24], who recorded 10 to 20 percent bandgap narrowing of graphene and metal oxides mixes that are optimized to work in solar collectors. The shifts are consistent with the results of layered material studies [25-26], which makes it clear that the integration of 2D materials enhances light absorption due to synergistic effects.

Devices fabricated by us achieve a PCE of 5.84 0.18, which is 63 percent higher than control devices. Comparatively, research achieved relative improvement in its efficiency (~50-70) using metal nanoparticle graphene hybrids in both dye solar cell and to a lesser extent polymer based; solar concentrations [27]. Efficiencies of ~60% have also been recorded by Mohammed *et al*. [21] by the use of graphene quantum dots in electron-transport layers. A combination of these findings shows that metallic nanoparticle-graphene hybrids have promise as avenues of increasing photon capture and charging in next-generation photovoltaics. [28-30-31]

The combined effects of rGO and metallic/oxide nanoparticles create manifold enhancements of electrical, thermal, and optical properties. These results are congruent with those of thermal engineering of hybrid composites[32-33] or the role of phonon engineering and conductive networks in improving the performance of the material. The agreement between our work and the literature space validates the claim that the nanocomposites of this nature bring about the extensive advantages to the solar energy conversion systems.

4. CONCLUSIONS

This research has proved that through its hybridization with zinc oxide (ZnO) and silver (Ag) nanoparticles the structural, optical, thermal and electrical properties of graphene oxide (GO) is increased significantly with improved electrical and thermal properties as a result of enhancing the hybridization between the nanoparticle and the GO. Optical absorption, narrowing of the band gap and thermal stability are significantly improved after the incorporation of the ZnO in the reduced GO matrix. Even more significant change is produced by addition of Ag nanoparticles to the rGO-ZnO matrix. The increase in conductivity is enormous, 1467 percent improvement, where the electrical conductivity of pure GO is found to be about 0.03 S/cm compared to the electrical conductivity of rGO-ZnO-Ag hybrid which is 0.47 \\pm 0.05 S/cm. This is ascribed to the combination of high surface area rGO and very good charge transport ability of metallic Ag nanoparticles, which provides a synergistic effect. Also, the output of the photovoltaic devices are improved dramatically. GO-based devices are posted 0.52 percent PCE, whereas rGO-ZnO has reported 2.18 percent and rGO-ZnO-Ag composites have attained a best performance of 3.41 percent that represent a 556 percent enhancement to the pure GO device. The

findings that are mentioned above, in terms of the raised short-circuit current density (0.91 mA/cm 2 to 4.27 mA/ cm^2), open-circuit voltage (0.33 V to 0.51 V), and fill factor (38.2% to 64.9%), confirm the important role of hybrid nanostructures in the improvement of solar cells. The present results support the perspective of rGO-ZnO-Ag nanocomposites to be a potential candidate to be used in the next-generation optoelectronic and energy conversion devices. The reduced graphene oxide, semiconducting ZnO and conductive Ag nanoparticles synergy offers a good platform in the tailoring of material properties to meet high-performance photovoltaics, sensors and photocatalysis.

References

[1] P. Jain, R.S. Rajput, S. Kumar, A. Sharma, A. Jain, B.J. Bora, ACS Omega 11 (2024) 12403.
[2] J. Wang, X. Mu, M. Sun, Nanomaterials 9 (2019) 218.
[3] P.J. Zhu, Y.N. Yan, Y. Zhou, Z.J. Qi, Y.F. Li, C.M. Chen, ACS Appl. Nano Mater. 7 (2024) 8445.
[4] T.A. Amollo, Heliyon 10 (2024) e26401.
[5] C. Anichini, P. Samorì, Small 17 (2021) 2100514.
[6] Z. Niazi, A. Hagfeldt, E.K. Goharshadi, J. Mater. Chem. A 11 (2023) 6659.
[7] E.T. Mombeshora, E. Muchuweni, R. Garcia-Rodriguez, M.L. Davies, V.O. Nyamori, B.S. Martincigh, Nanoscale Adv. 4 (2022) 2057.
[8] L.T. Siow, J.R. Lee, E.H. Ooi, E.V. Lau, Renew. Sustain. Energy Rev. 193 (2024) 114288.
[9] P. Kanti, K.V. Sharma, R.S. Khedkar, T.U. Rehman, Diam. Relat. Mater. 128 (2022) 109265.
[10] J. Qu, R. Zhang, L. Shang, Z. Wang, Int. J. Energy Res. 44 (2020) 7216.
[11] S.C. Kim, G. Poongavanam, S. Duraisamy, S. Parasuraman, M. Megaraj, Environ. Sci. Pollut. Res. 29 (2022) 8731.
[12] Aslfattahi, N., Saidur, R., Arifutzzaman, A., Abdelrazik, A. S., Samylingam, L., Sabri, M. F. M., & Sidik, N. A. C., J. Therm. Anal. Calorim. 147 (2022) 1125–1142.
[13] Z. Ali, S. Yaqoob, J. Yu, A. D'Amore, M. Fakhar-e-Alam, J. King Saud Univ. Sci. 36 (2024) 103457.
[14] A. Bafti, V. Mandić, I. Panžić, L. Pavić, V. Špada, ACS Nano 14 (2020) [pages pending].
[15] T. Venkatesh, S. Manikandan, C. Selvam, S. Harish, Int. Commun. Heat Mass Transf. 130 (2022) 105794.
[16] H.G. Abdulzahraa, M.K.A. Mohammed, A.S.M. Raoof, Surf. Interfaces 31 (2022) 102092.
[17] B.K. Mohammed, M.K.A. Mohammed, D.S. Ahmed, Mater. Today Energy 22 (2021) 100853.
[18] A.T. Al-Douri, R. Gdoura, Y. Al-Douri, A. Bouhemadou, A.F. Abd El-Rehim, J. Mater. Res. Technol. 15 (2021) 1487.
[19] Z. Barani, A. Mohammadzadeh, C.Y.T. Huang, L. Mangolini, F. Kargar, A.A. Balandin, arXiv preprint (2019).
[20] J.S. Lewis, Z. Barani, A. Sanchez Magana, F. Kargar, A.A. Balandin, arXiv preprint (2019).
[21] M.A.I. Rashed Al Mizan, M.A. Islam, Mater. Chem. Phys. 257 (2021) 123809.
[22] A. Nouri-Borujerdi, S. Kazemi-Ranjbar, Therm. Sci. Eng. Prog. 25 (2021) 100964.
[23] S.S. Safa, A.T. Al-Douri, A.A. Hadi, S.J.M. Alnajm, Exp. Theor. Nanotechnology. 9 (2025) 361.
[24] S. Aftab, M.Z. Iqbal, S. Hussain, H.H. Hegazy, M.A. Saeed, Nano Energy 108 (2023) 108249.
[25] P.K. Kanti, P. Sharma, M.P. Maiya, K.V. Sharma, Sol. Energy Mater. Sol. Cells 253 (2023) 112207.
[26] T.A. Amollo, Heliyon 10 (2024) [Article].
[27] Zhang, J.Y., Wu, X.B., & Shi, J.J., Phys. Chem. Chem. Phys. 26 (2024) 29584–29594.
[28] C.R. Chen, C. Chen, P.H. Cheng, W.H. Shi, T.P. Teng, Case Stud. Therm. Eng. 28 (2021) 101591.
[29] C. Liu, P. Lu, W. Chen, Y. Zhao, Y. Chen, Phys. Chem. Chem. Phys. 23 (2021) 26030.
[30] Y. Zhou, W. Qian, W. Huang, B. Liu, H. Lin, C. Dong, Nanomaterials 9 (2019) 1450.
[31] Maksood Adil Mahmoud Al-Doori1, Asaad T. Al-Douri1, Nahedh Ayad Faris. Exp. Theo. NANOTECHNOLOGY 9 (2025) 503
[32] Ahmed Suhail Hussein,Noor Khalid Ismael, Asaad T. Al-Douri, Abbas Saeb Zaham, Ali Y.Alwan1, Mais Qasem Mohammed, Sama Amer Abbas El-Tekreti, Shaimaa Tarik Mahmood, Saeb

Exp. Theo. NANOTECHNOLOGY 9 (2025) 571-589
Jasim Mohammed Alnajm,Younis W. Younis, Maksood Adil Mahmoud Al-Doori. Exp. Theo. NANOTECHNOLOGY 9 (2025) 512
[33] Safa Salah Salman, Asaad T. Al-Douri, Albosale Abbas Hadi,Saeb Jasim Mohammed Alnajm. Exp. Theo. NANOTECHNOLOGY 9 (2025) 372